Rev. Roum. Sci. Techn.– Électrotechn. et Énerg.
Vol. **66**, *1*, pp. 3–7, Bucarest, 2021

Électrotechnique et électroénergétique

PROCESSING, MICROSTRUCTURE AND MAGNETIC PROPERTIES OF ALNICO RIBBONS

EUGEN MANTA[1], EROS ALEXANDRU PATROI[1], DELIA PATROI[1*], ALEXANDRU IORGA[1*], GABRIELA SBARCEA[1], ANDREEA PETRE[1]

Key words: Alnico, Ribbons, Melt-spinning, Free-rare earth permanent magnets, Nanostructured alloy.

Since Alnico alloys are known as nanostructured metallic magnets, having a good corrosion and thermal stability, many research are devoted to find a miniaturization solution of this kind of permanent magnets in order to gain magnetic properties suitable to replace the permanent magnets containing critical elements, like Sm-Co and Nd-Fe-B permanent magnets, in the devices that requires lower performances and not so expensive routes for processing.
The experiments consisted in preparation of ribbons samples from Alnico based alloy processed in an induction furnace. From the obtained ingot, there where process ribbons by melt-spinning technique. The obtained ribbons where then heat-treated and characterized through X-ray diffraction (XRD), scanning electron microscopy (SEM) and vibrating sample magnetometer (VSM). The coercivity of the as-spun ribbons was enhanced from 16.92 kA/m to 32.57 kA/m after heat treatment.
A squarness ratio of around 0.6 is due the minor crystalline phases and to the residual stress induced by the rapid solidification process of the 2D structure of the ribbons, indicating a good candidate for radio-frequency identification (RFID), micro-electro-mechanical systems (MEMS) and other applications such as microwave circulators.

1. INTRODUCTION

The Al-Ni-Co alloy (normally abbreviated as Alnico) had become a significant milepost of permanent magnetic materials since it was first discovered by Mishima [1] in 1931, and it developed rapidly between the 1930s and 1960s. In the early 1960s, it was found that the microstructure formed by spinodal decomposition Alnico alloy was an important origin of high hard magnetic properties [2, 3]. Changing the preparation technologies can also effectively improve the magnetic properties. The traditional preparation processes of Alnico alloy mainly include three stages [4]. How to cheaply make the Alnico alloy lighter and thinner to cater for the rising requirement of precision instruments becomes a hard exciting subject in recent years. Lately, the Alnico ribbons melt-spun were produced by Konrad et al. [5], obtaining the maximum coercivity of 366 Oe (~29 kA/m), but the phase structure and magnetic properties caused by spinodal decomposition were not in depth studied.

The Alnico alloy first obtained the supersaturated α solid solution with body-centred cubic (BCC) structure by the solid-solution treatment. Then, the spinodal structure formed through the reaction of $\alpha \rightarrow \alpha_1+\alpha_2$ by the magnetic heat treatment (MHT) and multi-stage ageing, in which the α_1 phase is Fe–Co-rich ferromagnetic, and the α_2 is Al–Ni-rich weak ferromagnetic [6–10].

The interest in Alnico magnets is mainly due to their corrosion resistance and their use in devices that require high operating temperatures [11–13]. Radar and communication systems require low production costs and critical component dimensions when used in military applications. In such applications mainly used are microwave circulators and isolators, which typically consist of a ground plane, microwave ferrite and a permanent magnet. [14] These devices are critical in the switching and routing of microwave energy. Permanent magnets that are used are Sm-Co, due to high temperature stability and relatively high field strength, or Nd-Fe-B magnets. Since their production involve rare-earth critical elements and expensive cost production, Alnico-based ribbons can serve as good candidate for this kind of applications, taking into account their good thermal and chemical stability. Therefore, the study is devoted to processing and characterization of Alnico-based ribbons.

2. MATERIALS AND METHODS

The experiments consisted in preparation of samples, from Al-Ni-Co-Cu-Fe-Ti alloy with chemical composition as presented in Table 1. Melting and alloying was carried out in an induction furnace, Leybold-Heraeus type, starting from pure elements, namely: electrolytic Ni, Co, Cu (99.9 % purity), Ti, Al (technical purity), Fe (99.7 % purity). The samples where re-melted several times for the homogenization. From the ingot obtained in induction furnace, the alloy was ultra fast solidified, by melting in a melt-spinning installation, at speed of 26 m/s (Fig. 1). The obtained ribbons where then heat-treated at 850 °C for 30 minutes. The samples where cooled fast till 600 °C and another heat treatment was carried out at 600 °C for 5 hours. The process was repeated also by applying a magnetic field along the ribbons.

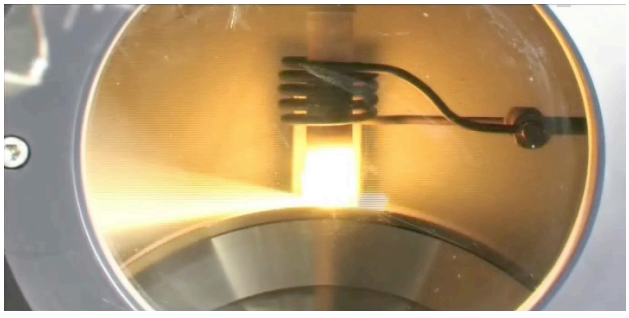

[1] National Institute for Research and Development in Electrical Engineering ICPE-CA (INCDIE ICPE-CA), Splaiul Unirii 313, sector 3, Bucharest, Romania
Corresponding author: delia.patroi@icpe-ca.ro, alexandru.iorga@icpe-ca.ro

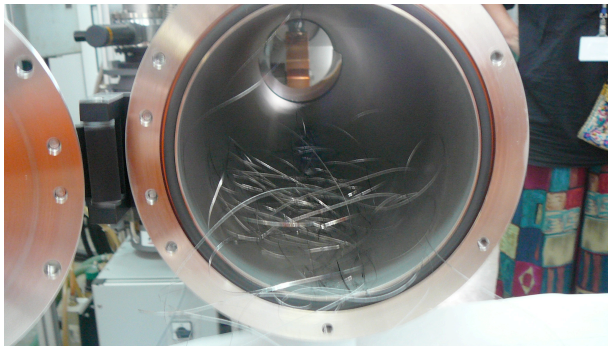

Fig. 1 – Aspects form casting Alnico alloys by melt spinning.

Table 1

Chemical composition of Alnico, (wt %)

Type of alloy	Chemical composition, wt%					
	Fe	Al	Ni	Co	Cu	Ti
Alnico	35.5	13.1	35.4	7.0	3.2	5.8

The chemical composition of the prepared alloys was investigated by EDS technique, on the FESEM-FIB Auriga integrated workstation.

The structure and the magnetic properties of the prepared alloys and compounds were investigated by SEM, XRD (using an X-ray diffractometer Bruker AXS D8 ADVANCE type), and magnetization measurements performed on vibrating sample magnetometer, 7300 Lake Shore type.

3. RESULTS AND DISCUSSION

3.1 XRD CHARACTERIZATION

The analysis by X-ray diffractometry was performed using the D8Discover diffractometer, Bruker-Germany, configured on primary optics with a tube with primary Cu radiation (λ = 1.540598Å), Göebel mirror and on secondary optics with a 1D LynxEye detector. Diffractograms were recorded in an angular increment of 0.04 ^{0} at a scan rate of 1 s/step. The qualitative analysis was performed using the ICDD Release 2015 database. Considering the main crystallographic phases, the Rietveld analysis determined the parameters of the elementary cell, respectively the average crystallite size.

Figure 2 (a) shows the experimental diffractogram of the obtained sample. The qualitative analysis highlights the presence of the main crystallographic phases of $Al_{0.42}Ni_{0.58}$ (at %) cubic crystallized, belonging to the space group Pm-3m (221), according to the PDF file no. 00-044-1267, of an additional phase of $Fe_{0.51}Co_{0.24}Ni_{0.14}Al_{0.08}Cu_{0.03}$ (at %), associated with the theoretical PDF file 01-074-6458 with the cubic structure with centred volume belonging to the space group Im-3m (229), respectively the presence of some residual/intermediate phases of Co_3B (at %), $Al_{12.1}(Co_{0.88}Ni_{0.12})_4$ (at %), and $(Al_{0.17}Co_{0.5}Ti_{0.33})Co_3$ (at %) represented as a minority in the experimental diffractogram.

From a semi-quantitative point of view, the Rietveld analysis highlighted the presence of over 90 % $Al_{0.42}$ $Ni_{0.58}$ (at %) phase characterized by the presence of diffraction maxima at 2θ angular positions: 31.02 °, 44.44 °, 64.66 °, 81.84 ° and 98.29 °, associated with the crystalline planes

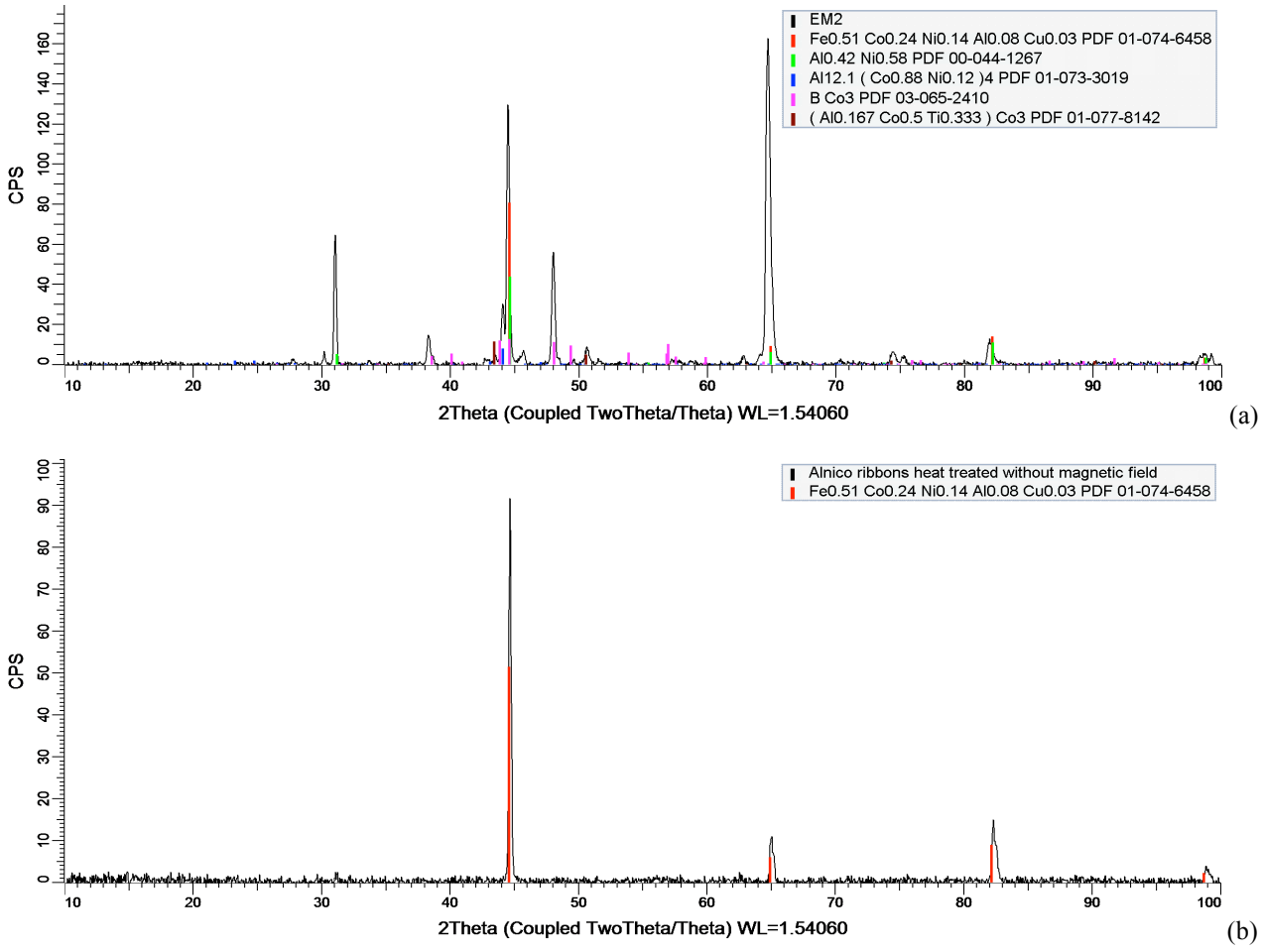

Fig. 2 – XRD analysis of Alnico ribbons as obtained (a) and heat-treated without magnetic field (b).

(001), (011), (002), (211) and (022) respectively.

The average crystallite size D = 59 nm, respectively the elementary cell parameter a_{exp} = 2.881Å were determined by Rietveld analysis related to a cubic structure with centred volume belonging to the space group Pm-3m (221) with the elementary cell parameter theoretically a_{teor} = 2.871Å. The additional phase of $Fe_{0.51}$ $Co_{0.24}$ $Ni_{0.14}Al_{0.08}Cu_{0.03}$ (at %) shows the parameter of the elementary cell close in value to that of the main phase, a_{exp} = 2.907Å.

After heat-treatment, the ribbons contain only the main cubic crystalline phase of $Fe_{0.51}Co_{0.24}Ni_{0.14}Al_{0.08}Cu_{0.03}$ preferential oriented on [220] direction without secondary phases (Fig. 2 (b)). The average crystallite size D = 95 nm, respectively the elementary cell parameter a_{exp} = 2.868Å were determined by Rietveld analysis and suggest the development of the principal crystalline phase with a residual stress on its lattice.

3.2 MICROSTRUCTURE OF THE SYNTHESIZED MATERIALS

Scanning electron microscopy was performed with the Auriga model workstation produced by Carl Zeiss SMT Germany FESEM-FIB with Gemini column field emission source for the electron beam. For the morphology, the Everhart Thornley SESI secondary electron detector with the Faraday cup in the test chamber was used. The energy dispersive spectrometric analysis was performed by the XmaxN probe and Aztec software.

The samples were analysed without other mechanical or chemical processing (after being attached to the aluminium support with the help of a carbon conductive strip)

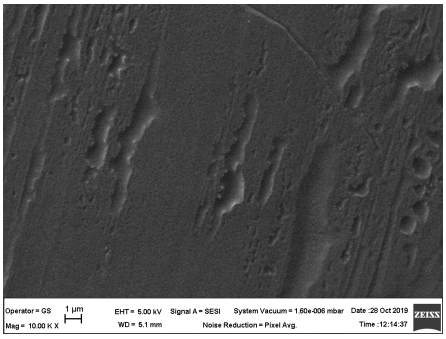

(a)

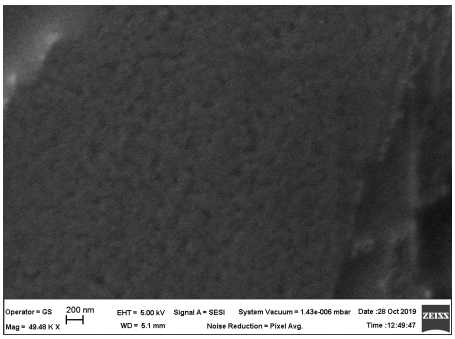

(b)

Fig. 3 – Microstructure of Alnico ribbons; face down surface of the ribbons (contact with the rotating drum) (a) morphology at 10000x magnification, (b) morphology at 50000x magnification.

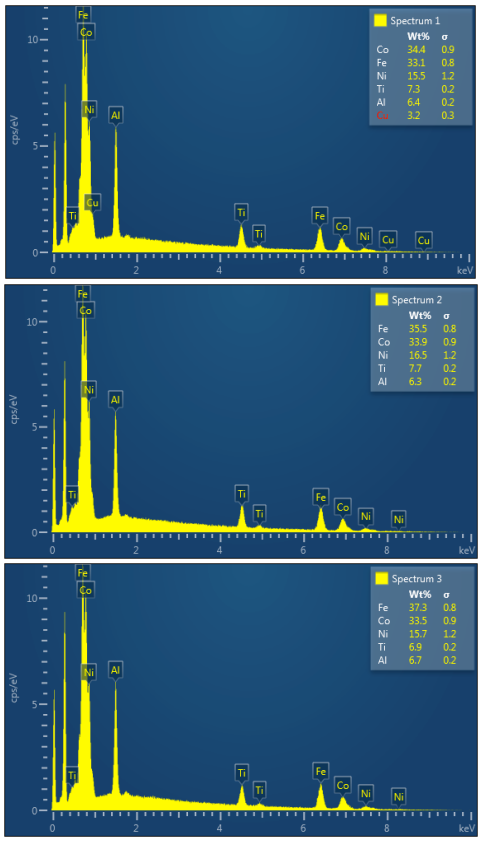

Fig. 4 – Alnico ribbons – EDS of face down surface of the ribbons (contact with the rotating drum) on different micro-areas.

The SEM images (Fig.3) show a uniform morphology with a refined structure without clearly highlighted crystals. No topographic differences are observed, suggesting that the sample has a uniform thickness, the surface defects being the result of the casting process, since the ribbons replicate the surface of the rotating drum.

The energy-dispersive X-ray spectroscopy (EDS) analysis (Fig. 4) shows an elementary chemical composition based on Fe-Co with Ti, Al, Ni and Cu additive elements. There were observed slightly differences in elemental composition by the analysis of different micro-areas, Cu element being present just in one analysed region. This can be explained by the low content of Cu in the main alloy used for producing the ribbons and its presence in some specific regions is normal since it is used as initiating crystallization centres.

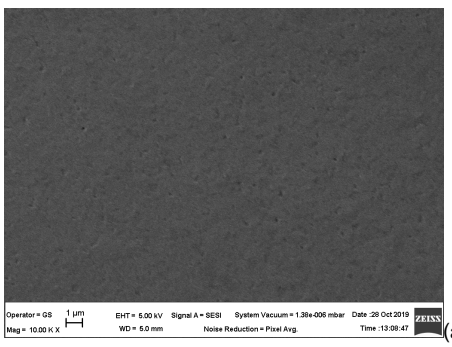

(a)

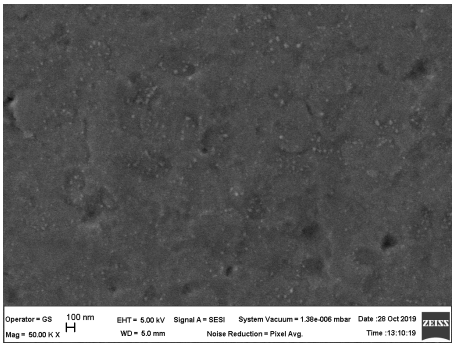

(b)

Fig. 5 – Microstructure of Alnico ribbons – face up surface of the ribbons (no contact with the rotating drum) (a) morphology at 10000x, (b) morphology at 50000x magnification.

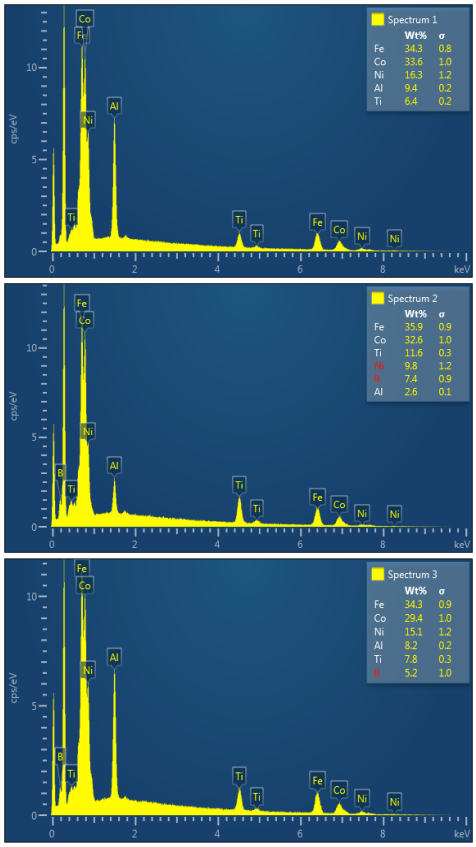

Fig. 6 – Alnico ribbons – EDS of face up surface of the ribbons (no contact with the rotating drum) on different micro-areas.

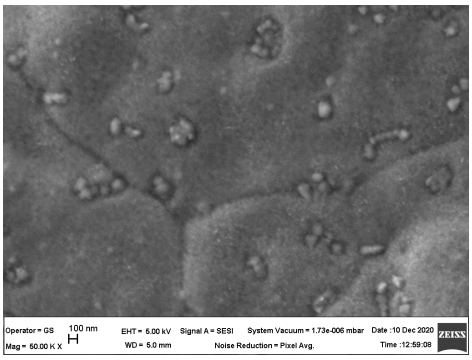

Fig. 7 – Microstructure of heat-treated Alnico ribbons; face up surface of the ribbons (no contact with the rotating drum) morphology at 50000x magnification.

The SEM images (Fig. 5) show a uniform morphology with a fine structure with the appearance of nanocrystals. Some thin fractures are present over the surface due to the rapid crystallization process in ribbon production process.

The EDS analysis (Fig. 6) shows an elementary chemical composition based on Fe-Co with Ti, Al, Ni, and Cu additive elements. Also, it was noticed the presence of some B contaminants due to the interaction of the main alloy with the crucible used for initial melting process. This element slightly contributes also to the crystalline phases identified by X-ray analysis.

After heat treatment the ribbons presented large grain structure with some crystals decorations at about 100 nm, as presented in Fig. 7. EDS showed no differences in chemical composition with respect of the as-cast ribbons.

3.3 MAGNETIC PROPERTIES

A widely experimental method, which can give all the necessary data for the material model identification, is based on the Vibrating Sample Magnetometer (VSM), very sensitive equipment, which uses small samples and can generate large magnetic fields (10^6 A/m) in a small air-gap (a few millimetres) [15].

The magnetic measurements were performed with the VSM LAKE SHORE vibrating sample magnetometer model 7300, at room temperature. The measurements were performed on the same sample before and after thermal annealing with following dimensions: 5 mm long, 1.5 mm wide and 35 μm thick. In order to correct the hysteresis loops it was considered a demagnetization factor for the 1.5/5 ratio, N_m = 0.69 [16]. The hysteresis curves are presented in Fig. 8 and Fig. 9. The main magnetic characteristics, the magnetization at saturation M_s, the remanent magnetization M_r and the coercive field are presented in Table 2.

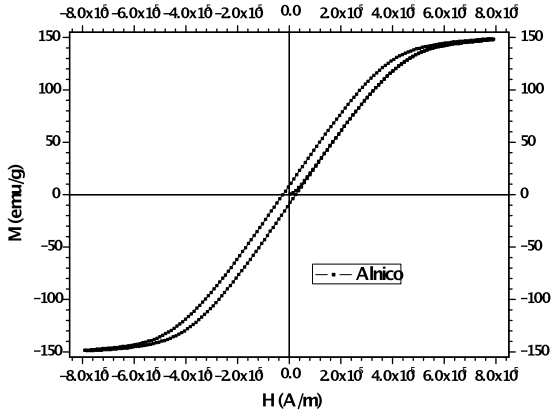

Fig. 8 – Hysteresis curves of Alnico as-cast.

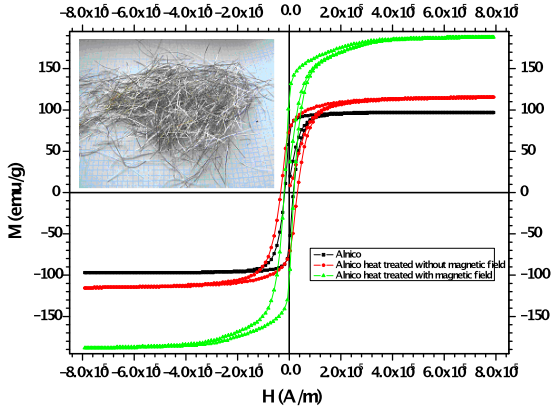

Fig. 9 – Hysteresis curves of Alnico ribbons.

Table 2

The main magnetic characteristics of the studied alloys

No.	Sample code	Remanent magnetisation, M_r [emu/g]	Saturation magnetisation, M_s [emu/g]	Coercivity, H_c [kA/m]
1	Alnico as-cast	9.17	150.35	24.25
2	Alnico ribbons	63.8	97	16.92
3	Alnico ribbons heat treated without magnetic field	74.8	115	32.57
4	Alnico ribbons heat treated in magnetic field	109	188	18.86

The room temperature coercivity of the as-spun ribbons was enhanced from 16.92 kA/m to 32.57 kA/m after heat treatment. The magnetic properties were measured after heat treatment with and without applying magnetic field. For the Alnico ribbons heat-treated without magnetic field we obtain a better H_c than with magnetic field heat treatment, but slightly higher M_s and M_r.

Considering the coercivity values for the Alnico ribbons heat-treated without magnetic field, this kind of ribbons can be used for MEMS. Further, the Alnico ribbons heat-treated in magnetic field can be good candidates for RFID applications.

4. **CONCLUSIONS**

Alnico ribbons having a main crystallographic phases of cubic $Al_{0.42}Ni_{0.58}$ (at %), additional phases of fcc $Fe_{0.51}Co_{0.24}Ni_{0.14}Al_{0.08}Cu_{0.03}$(at%), and residual phases of Co_3B (at%), $Al_{12.1}(Co_{0.88}Ni_{0.12})_4$ (at %), $(Al_{0.17}Co_{0.5}Ti_{0.33})Co_3$ (at %) were subjected to the analysis of the magnetic properties behaviour over the annealing process. Considering the uniform morphology of the ribbons, observed by SEM and the cubic structure of the main crystalline phases of the ribbons it is expected a magnetic isotropic behaviour of the ribbons. The crystalline arrangement of the Alnico ribbons it quite different compared to the as already known Alnico permanent magnets, since no occurrence of hard magnetic FeCo-rich crystalline phase was identified. The main identified crystalline phases rather contribute to a soft (semi-hard) magnetic behaviour. Even the squarness ratio M_r/M_s of the heat treated it is ten times higher compared to the as cast Alnico, the coercivity it is slightly improved only when the ribbons are annealed without the presence of magnetic field. This can suggest that the presence of the magnetic field does not influence the orientation of some crystalline phases to improve the coercivity by shape anisotropy, like are developed the Alnico permanent magnets. Since a M_r/M_s of 0.5 it is considered in literature for non-interacting uniaxial single domain particles with randomly easy axis orientation, it is possible that for the heat-treated ribbons, with a squarness ration of around 0,6 to have a slightly induced interaction due to the presence of the minor crystalline phases and to the residual stress induced by the rapid solidification process and the 2D structure of the ribbons.

The short time of the thermo-magnetic treatment did not lead to the improvement of the magnetic properties. Future research will focus on the influence of thermo-magnetic treatment times and their magnetic properties behaviour in frequency.

ACKNOWLEDGEMENT

The work has been funded by the Nucleu Programme, PN 19310103/2019, and the Bilateral Cooperation with DUBNA contract 85/2019. The project 30PFE/2018 is acknowledged for providing the infrastructure used in this work.

Received on January 7, 2021

REFERENCES

1. J. Ormerod, *Permanent magnet materials*, IEEE Trans. Magn. **4**, pp. 84–99 (1968).
2. F. Zhu, L.V. Alvensleben, P. Haasen, *A study of Alnico magnets by atom probe field ion microscopy*, Scr. Metall. **18,** pp. 337–342 (1984).
3. W.G. Chu, W.D. Fei, X.H. Li, D.Z. Yang, *A study on the microstructure of Alnico alloy thermomagnetically treated at various temperatures*, Mater. Chem. Phys., **73,** pp. 290–294 (2002).
4. Y.L. Sun, J.T. Zhao, Z. Liu, W.X. Xia, S.M. Zhu, D. Lee, A.R. Yan, *The phase and microstructure analysis of Alnico magnets with high coercivity*, J. Magn. Magn.Mater. **379**, pp. 58–62 (2015).
5. K. Löwe, M. Dürrschnabel, L. Molina-Luna, R. Madugundo, B. Frincu, H.J.Kleebe, O. Gutfleisch, G.C. Hadjipanayis, *Microstructure and magnetic properties of melt-spun Alnico-5 alloys*, J. Magn. Magn. Mater. **407**, pp. 230–234 (2016).
6. R.A. McCurrie, *Chapter 3 The structure and properties of Alnico permanent magnet alloys*, in: E.P. Wohlfarth (Ed.), Handbook of Ferromagnetic Materials, Elsevier, pp. 107–188 (1982).
7. J. Mohapatra, M. Xing, J. Elkins, J.P. Liu, *Hard and semi-hard magnetic materials based on cobalt and cobalt alloys*, J. Alloys Compd. **824**, *153874* (2020).
8. X.Y. Sun, C.L. Chen, M.Y. Ma, L. Yang, L.X. Lv, S. Atroshenko, W.Z. Shao, L. Zhen*, Structure and magnetic properties of Alnico8 alloy thermo-magnetically treated under a 10 T magnetic field, Intermetallics*, **119**, *106691*, (2000).
9. W. Schäfer, E. Jansen, W. Kockelmann, A. Alker, A. Kirfel, D. Seitz, M. Gr ̈onefeld, *Variations of microstructure and texture of permanent magnetic Alnico alloys*, Physica **B**, *276–278*, pp. 866–867 (2000).
10. S.U. Rehman, Q. Jiang, W. Lei, K. Liu, L. Zeng, M. Ghazanfar, T. Ahmad, R. Liu, S. Ma, Z. Zhong, *Microstructures and magnetic properties of cast Alnico 8 permanent magnets under various heat treatment conditions*, Physica B **552**, pp. 136–141 (2019).
11. J. Cui, M. Kramer, L. Zhou, F. Liu, A. Gabay, G. Hadjipanayis, B. Balasubramanian, D. Sellmyer, *Current progress and future challenges in rare-earth-free permanent magnets*, Acta Mater. **158**, pp. 118–137 (2018).
12. E.M.H. White, A.G. Kassen, E. Simsek, W. Tang, R.T. Ott, I.E. Anderson, *Net shape processing of Alnico magnets by additive manufacturing*, IEEE Trans. Magn. **53**, pp. 1–6 (2017).
13. J.M.D. Coey, *Perspective and prospects for rare earth permanent magnets, Engineering* **6**, pp. 119–131 (2020).
14. L. Martinez, V. Laur, A. L. Borja, P. Quéffélec, A. Belenguer, *Low Loss Ferrite Y-Junction Circulator Based on Empty Substrate Integrated Coaxial Line at Ku-Band*, IEEE Access, **7**, pp. 104789-104796 (2019).
15. V. Ioniţă, L. Petrescu, *Magnetic material characterization by open sample measurements*, Rev. Roum. Sci. Techn.– Électrotechn. et Énerg., **54**, *1*, pp. 87–94, Bucharest (2009).
16. D.-X. Chen and C. Prados, E. Pardo, A. Sanchez, A. Hernando, *Transverse demagnetizing factors of long rectangular bars: I. Analytical expressions for extreme values of susceptibility*, J. of Applied Physics, **91**, *8*, pp. 5254 – 5259 (2002).